Journal of Saudi Chemical Society (2019) **23**, 636–641

King Saud University

Journal of Saudi Chemical Society

www.ksu.edu.sa
www.sciencedirect.com

ORIGINAL ARTICLE

Pyridine solvated dioxouranium complex with salen ligand: Synthesis, characterization and luminescence properties

Mohammad Azam [a,*], Saud I. Al-Resayes [a], Agata Trzesowska-Kruszynska [b], Rafal Kruszynski [b], S.F. Adil [a], N.K. Lokanath [c]

[a] *Department of Chemistry, College of Science, King Saud University, P.O. Box 2455, Riyadh 11451, Saudi Arabia*
[b] *Institute of General and Ecological Chemistry, Lodz University of Technology, Zeromskiego 116, 90-924 Lodz, Poland*
[c] *Dept. of Studies in Physics, University of Mysore, Manasagangotri, Mysore 570 006, India*

Received 13 July 2018; revised 22 January 2019; accepted 24 January 2019
Available online 10 February 2019

KEYWORDS

Uranyl complex;
Crystal structure;
Photoluminescence

Abstract A new derivative of dioxouranium(VI) salen complex, [UO2(L)(pyridine)], where [L = N,N′-Bis(2-hydroxybenzylidene)-2,2-dimethyl-1,3-propanediamine] is synthesized and characterized by elemental analysis (C, H, N), FT-IR, ESI-MS spectrometry, UV/Vis, fluorescence, ^{1}H and ^{13}C NMR spectroscopy and thermal gravimetric (TG) study. Furthermore, the single crystal X-ray diffraction measurements of the complex were carried out at 100 and 273 K. The crystal structure measurements revealed that the complex has distorted pentagonal bipyramidal geometry with uranium atom located at the centre and bonded to two phenoxy oxygen and two azomethine nitrogen in tetradenate fashion and one nitrogen from pyridine making it seven coordinated. In addition, the photoluminescence property of the complex was also recorded.

1. Introduction

The hexavalent uranyl ion (UO_2^{2+}) is the most abundant linear functional unit in the chemistry of uranium containing complexes due to the remarkable stability of its oxo groups at the apical position [1–6]. The robust nature of uranyl ion arises due to the strong interaction between 2p orbital of oxygen and 5f/6d orbitals of uranium [1,6–9].

Over the years, uranium complexes have shown significant reactivity with various unprecedented applications, such as photochemistry, gas sorption, ion-exchange, selective oxidation catalysis, photochemical reduction, axial uranium-oxygen bond activation and several others [10–14].

Herein, we are concerned to report the synthesis of a derivative of a new pyridine solvated mononuclear uranyl complex [UO_2L(Pyridine)], and its characterization by elemental analysis, FT-IR, UV/Vis, fluorescence, ^{1}H and ^{13}C NMR spectroscopy and thermogravimetric (TG) analysis. In

* Corresponding author.
E-mail address: azam_res@yahoo.com (M. Azam).
Peer review under responsibility of King Saud University.

Production and hosting by Elsevier

https://doi.org/10.1016/j.jscs.2019.01.006
1319-6103

Table 1 Crystal and structure refinement data of uranyl compound.

Temperature	100 K	293 K
Empirical formula	$C_{24}H_{25}N_3O_4U$	$C_{24}H_{25}N_3O_4U$
Formula weight	657.50	657.50
Crystal system, space group	monoclinic, *I* 2/*a* (No.15)	monoclinic, *I* 2/*a* (No.15)
Unit cell dimensions [Å, °]	$a = 11.9209(14)$	$a = 12.021(7)$
	$b = 14.1724(18)$	$b = 14.299(4)$
	$c = 13.398(2)$	$c = 13.569(12)$
	$\beta = 97.118(12)$	$\beta = 97.070(14)$
Volume [Å^3]	2246.1(5)	2314(2)
Z, Calculated density [Mg/m^3]	4, 1.944	4, 1.887
F(0 0 0)	1256	1256
Crystal size [mm]	0.093, 0.091, 0.018	0.093, 0.091, 0.018
θ range for data collection [°]	4.560 to 67.004	3.416 to 25.031
Index ranges	$-13 \le h \le 14$, $-16 \le k \le 16$, $-15 \le l \le 15$	$-14 \le h \le 14$, $-16 \le k \le 15$, $-6 \le l \le 15$
Reflections collected/unique	11,415/2002 [$R_{(int)} = 0.0341$]	3540/2037 [$R_{(int)} = 0.2487$]
Completeness [%]	100 (to $\theta = 67°$)	99.0 (to $\theta = 25°$)
Data/restraints/parameters	2002/0/150	2037/0/148
Goodness-of-fit on F^2	1.148	1.184
Final *R* indices [$I > 2\sigma(I)$]	$R1 = 0.0334$, $wR2 = 0.0914$	$R1 = 0.1341$, $wR2 = 0.3220$
R indices (all data)	$R1 = 0.0334$, $wR2 = 0.0914$	$R1 = 0.1371$, $wR2 = 0.3307$
Largest diff. peak and hole [e Å^{-3}]	1.423, −5.908	8.374, −8.100

addition, the single crystal X-ray diffraction measurements at 100 and 273 K were also recorded to reveal the structural properties.

2. Experimental

2.1. Chemicals and instruments

2,2-Dimethyl-1,3-propanediamine (99% purity), 2-hydroxybenzaldehyde (98% purity), ethanol (99.8% purity) were procured from Sigma–Aldrich. Uranyl acetate dihydrate (98% purity) and Pyridine (99.5% purity) were purchased from BDH lab reagents and Qualikems Chemicals, respectively. Elemental microanalyses (CHN) were obtained using a Elementar Varrio EL analyser. UV/Vis and FT-IR spectra were recorded on Pharmacia LKB-Biochem spectrophotometer and Perkin Elmer 621 infrared spectrophotometer, respectively. ^{1}H NMR and ^{13}C NMR (100 MHz) spectra were recorded on JEOL-400 spectrometer in d_6-DMSO.

2.2. Synthesis of a pyridine solvated dioxouranium(VI) salen complex [UO_2 (L)(Py)]

Uranyl acetate (0.7 mmol, 300 mg) was slowly added into a solution of H_2L (0.7 mmol, 219 mg) [15] dissolved in 10 ml pyridine. The resultant reaction mixture was stirred for 5 h leading to colour change from yellow to orange. The orange coloured solution yielded crystalline product upon evaporation at room temperature within a week.

Yield 65.8%, mp. 241 °C; molecular formula $C_{24}H_{25}N_3O_4U$; Anal Calc. C, 43.84; H, 3.83; N, 6.39%; Found: C, 43.28; H, 3.85; N, 6.33%. ^{1}H NMR (DMSO d_6): δ (ppm) 9.26 (s, **—**CH═N), 6.68–8.58 (m Ph-**H**), 3.36 (s, 4H, –C**H$_2$**), 1.26 (s, 6H, (–C(C**H$_3$**)$_2$**), ^{13}C NMR (DMSO d_6, 100 MHz): 169.9 (**—C**H═N), 39.8 (**C**–(CH$_3$)$_2$), 24.8 (**C**H$_3$)$_2$–C), 69.1 (–**C**H$_2$-); 116.8–150.0 (**C**-Ph); IR (KBr, cm^{-1}) 1615 $\nu_{(-CH=N)}$, 1211 $\nu_{(Ph-O)}$.

2.3. Crystal structure determination

The X-ray intensity data for the orange prismatic crystals of [UO_2(L)Py] were collected with graphite monochromated CuK_α ($\lambda = 1.54178$ Å) radiation at temperature 100.0(1) K and MoK_α ($\lambda = 0.71073$ Å) radiation at temperature 293.0(1) K on a Bruker APEX2 automatic diffractometer equipped with CCD detector. In both measurements, the ω scan mode was applied and the 6 s exposure time was used. The reflections inside Ewald sphere were collected up to $\theta = 67°$ at 100.0(1) K and up to $\theta = 25°$ at 293.0(1) K. The details concerning crystal data and refinement are given in Table 1. During the data

Table 2 Selected structural data of uranyl complex [Å, °].

Temperature	100 K	293 K
U1–O1	2.247(5)	2.249(14)
U1–O2	1.789(6)	1.797(18)
U1–N1	2.582(6)	2.61(3)
U1–N2	2.582(6)	2.589(18)
N1–C7	1.282(10)	1.33(3)
N1–C8	1.466(9)	1.44(3)
O2–U1–O2^i	177.5(3)	179.3(8)
O2–U1–O1^i	89.4(2)	87.0(7)
O2–U1–O1	91.2(2)	93.2(7)
O1–U1–O1^i	148.9(3)	150.0(7)
O2–U1–N2	91.24(14)	90.3(4)
O1–U1–N2	74.43(13)	75.0(4)
O2–U1–N1	87.3(2)	88.8(6)
O1–U1–N1	69.88(19)	69.6(5)
N2–U1–N1	144.23(14)	144.4(4)
O2–U1–N1^i	90.7(2)	90.7(6)
O1–U1–N1^i	141.22(19)	140.4(5)
N1–U1–N1^i	71.5(3)	71.2(8)

Symmetry transformations used to generate equivalent atoms: (i) −x + 1/2, y, −z.

Table 3 Stacking interactions [Å, °]. $C_g(1)$ and $C_g(2)$ indicate the centroids of six-membered aromatic rings (R) containing C1, N2 atoms respectively, α is a dihedral angle between planes I and J, β is an angle between Cg(I)-Cg(J) vector and normal to plane I and d_p is a perpendicular distance of Cg(I) on ring J plane.

R(I)···R(J)	Cg···Cg	α	β	d_p
100 K				
Cg(2)···Cg(1)^{ii}	3.7245	10.898	27.90	3.5281
Cg(2)···Cg(1)^{iii}	5.8148	10.898	58.75	2.0344
Cg(1)···Cg(2)^{iv}	3.7245	10.898	18.69	3.2915
273 K				
Cg(2)···Cg(1)^{ii}	3.7904	12.407	29.54	3.6065
Cg(2)···Cg(1)^{iii}	5.9024	12.407	57.87	2.0494
Cg(1)···Cg(2)^{iv}	3.7904	12.407	17.92	3.2977

Symmetry transformations used to generate rings: (ii) −x,1 − y,−z and 1/2 + x,1 − y,z; (iii) 1/2 + x,1/2 + y,−1/2 + z and −x,1/2 + y,1/2 − z; (iv) −x,1 − y,−z and −1/2 + x,1 − y,z.

reduction, the Lorentz, polarization and empirical absorption [16] corrections were applied.

The XS, XL and XTL [17] programs were employed in all calculations, where XTL consist of all major programs describing the structure. The XS is employed for Structure solution by "phase annealing" direct methods, and XL is for Least-square structure refinement. The selected interatomic bond distances and angles are listed in Table 2 and intermolecular interactions are listed in Table 3. The electron density of uranium cation in studied compound shows extreme anisotropy. It leads to formation of multiple difference Fourier peaks and holes around uranium cation, in both is anisotropic and isotropic refinements. In the measurements performed at 100 K, this effect leads subsequently to collapsing of structural anisotropic displacement parameters along two fold axis and falling of the orthogonalized values out of real part of Euclidean metric space. To check the possibility of larger uniformity of electron density of uranium cation at temperatures greater than used in measurement (100 K), the sample was re-measured at 293 K. Generally, increasing the temperature leads to expansion of atomic electron density and flattening of its shape and, thus, the re-measurement could lead to decreasing of anisotropic character of electron density of uranium cation. The measurement at 293 K shows that mutual effects of anisotropy of electron density of uranium cation are the same as observed in the measurement performed at 100 K. Due to electron density expansion, the displacement ellipsoids were normal, but the match between the calculated and experimental densities was distinctly worse than that of the measurement at 100 K. Nevertheless of the above, in both cases, the molecular geometry (including bond distances and interbond angles) was the same and the model correctly represents the atom placements and linkage.

3. Results and discussion

The molecular structure of pyridine solvated uranyl complex is given in Fig. 1. The uranyl complex possesses a doubly deprotonated tetradentate chelating ligand [15], UO_2^{2+} ion and a uranium coordinated pyridine molecule. The U1, C9, N2 C13 and H13 atoms occupy special positions *e* of *I2/a* space group with site symmetry 2 and multiplicity 4, and, thus, one molecule is located in two asymmetric units. This phenomenon

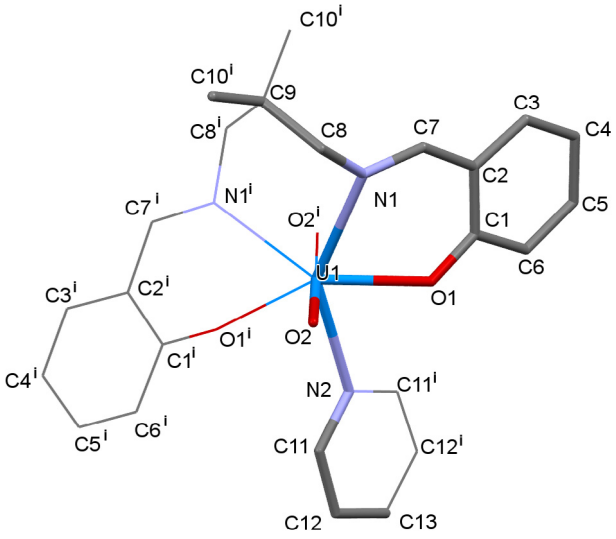

Fig. 1 The molecular structure of pyridine solvated uranyl complex. The symmetry-generated part is indicated by thin bonds. Symmetry code: (i) −x + 1/2, y, −z.

is analogous to that in THF coordinated uranyl complex reported in the literature and similar to pseudosymmetry twofold rotation axis observed in ethanol coordinated uranium complex [18]. The (N,N′-bis(salicylidene)-2,2-dimethyl-1,3-propanediaminato)-dioxouranium(VI) moiety in both above mentioned uranium compounds possesses very similar conformation, and the root mean square deviation of superimposed moieties is not lager than 0.3 for each pair of moieties. The uranium atoms are seven coordinated by two imine nitrogen atoms, two alkoxide oxygen atoms, two oxide oxygen atoms and one nitrogen atom of N-heterocyclic molecule, making geometry slightly distorted pentagonal bipyramid [18] with the oxide oxygen atoms located at the polyhedron apices. The studied compound is the first example of N′-bis(2-hydroxy benzylidene)-2,2-dimethyl-1,3-propanediamine in the preparation of N_3O_4 coordination sphere with coordination number 7. So far, this ligand has been used in preparation of several coordination compounds of varying coordination number [19] or form N_2O_5 coordination sphere [20]. The salicylidene-1-methaneaminato moieties are distorted from planarity [15] due to the coordination with relatively large uranyl ion.

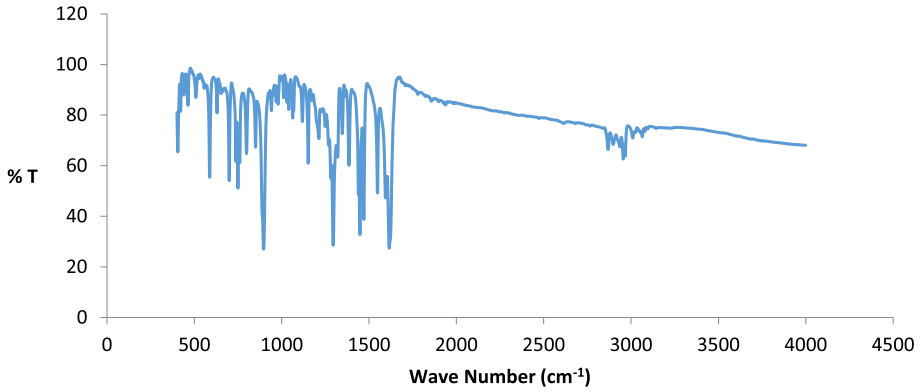

Fig. 2 FT-IR spectrum of uranyl complex.

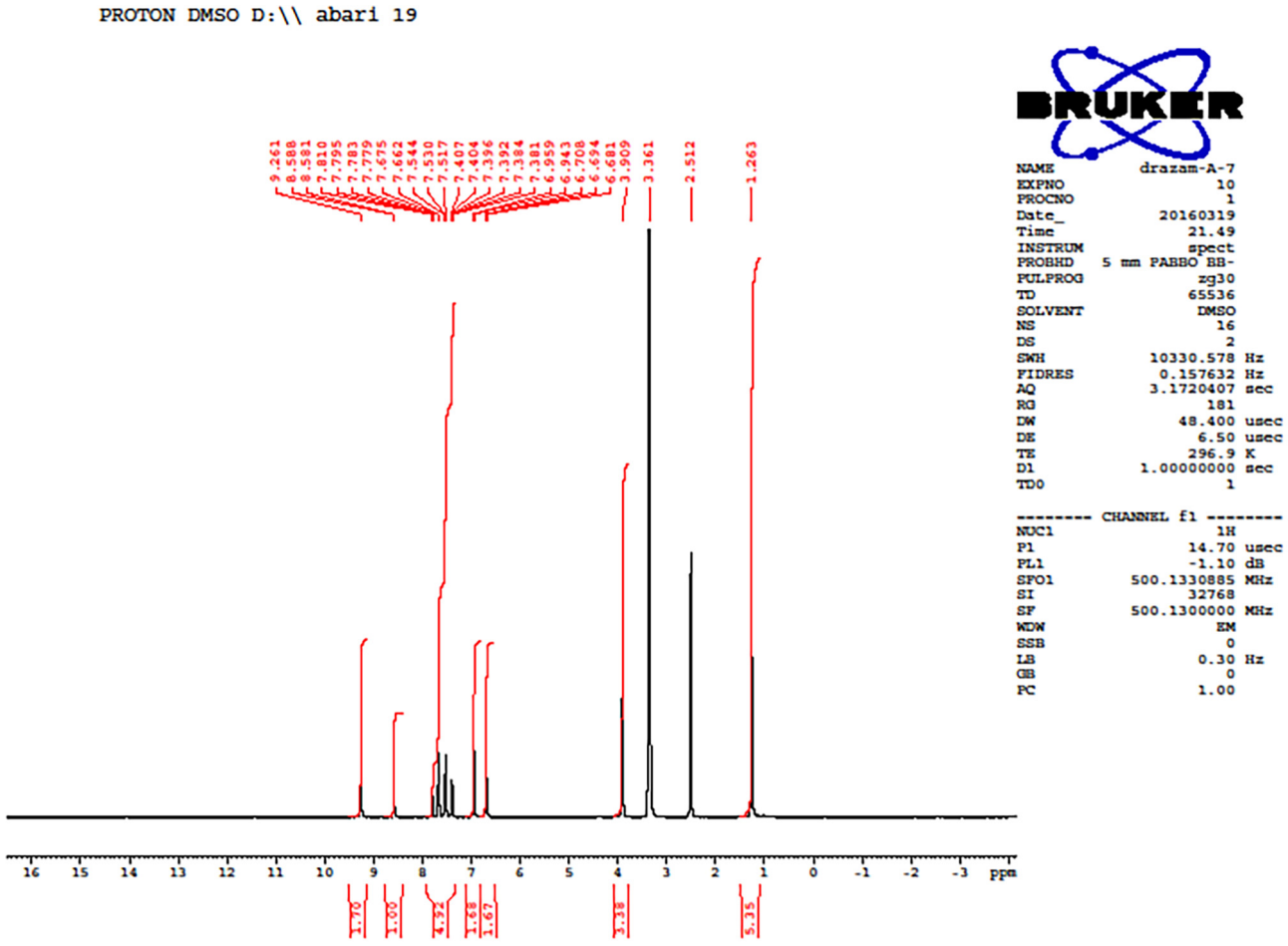

Fig. 3 ^{1}H NMR spectrum of uranyl complex.

The molecules of studied compound do not create any hydrogen bond, even the non-classical ones [21]. It is uncommon situation because even in absence of classical hydrogen bond donors, the C–H donors typically create some weak hydrogen bonds linkage in presence of oxygen atoms, which can serve as acceptors [22]. The presence of aromatic six-membered rings, rich in π electrons, causes formation of three pairs of π···π interactions (Table 3) [23]. Each symmetry depends on pair links to neighbouring molecules to the piles extending along [1 0 0] [0 0 1] [10 –1] crystallographic axes. These linkages lead to formation of the π···π three-dimensional supramolecular network.

3.1. Spectroscopy

The prominent bonding in the studied uranyl complex has been ascertained on the basis of FT-IR spectrum [Fig. 2]. The characteristic band due to $\nu_{(-CH=N)}$ group vibration

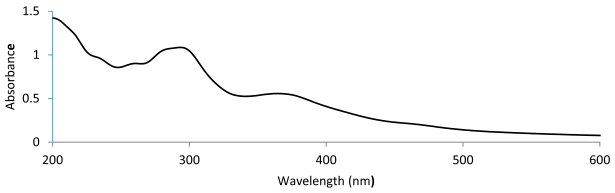

Fig. 4 UV/Vis spectrum of uranyl complex.

appears at 1615 cm^{-1} [24,25], which gets further confirmation by the presence of $\nu_{(U-N)}$ vibrations at 587 cm^{-1} [24,25]. Furthermore, the $\nu_{(Ar-O-U)}$ vibrations at 1211 cm^{-1} indicate the coordination of uranyl ion to the phenolic oxygen atoms [26,27]. In addition, the phenyl ring vibrations appear at 695 cm^{-1}, 1030 cm^{-1} and 1470 cm^{-1} [24,25]. The bending vibrations due to symmetric and asymmetric alkyl group are observed at 1474 cm^{-1} and 1367 cm^{-1}, respectively, whereas the vibration due to $\nu_{(CH3)2C-}$ group is revealed at 1151 cm^{-1} [28]. The uranyl vibrations are noticed at 750 cm^{-1}, 798 cm^{-1} and 850 cm^{-1} [29], whereas the pyridine ring vibrations at 421–440 cm^{-1} and 629–652 cm^{-1} [30].

The ^{1}H NMR spectrum of uranyl complex exhibits all signals belonging to aliphatic and aromatic protons [Fig. 3]. The most characteristic signal attributed to azomethine proton appeared at 9.26 ppm, whereas the chemical shifts for aromatic protons were found at 6.68–8.58 ppm. A sharp singlet due to methyl protons of (–C($\mathbf{CH_3}$)$_3$) group appeared at 1.26 ppm, whereas the broad multiplet due to –CH_2 proton was observed at 3.36 ppm.

The ^{13}C NMR spectrum of uranyl complex revealed the expected number of carbon signals equivalent to different type of carbon atoms present in the complex. The azomethine and aromatic carbon signals appeared at 169.9 ppm and 116.8–150.0 ppm, respectively. Furthermore, the –CH_2 carbon peaks were noticed at 69.1 ppm, whereas the –CH_3 and quaternary carbon appeared at 24.8 ppm and 39.8 ppm, respectively.

The UV/vis spectrum of the complex revealed the absorption band at 200–300 nm due to π–π^* transition of the phenyl ring and azomethine group [Fig. 4] [31]. The absorption band at 452 nm ($\varepsilon = 2.1 \times 10^5$ M^{-1} cm^{-1}) is due to LMCT transitions, and this feature is assigned to f-d or charge-transfer transitions [32–34].

The ESI-MS spectrum of the complex revealed the presence of a cation adduct, $[M + Na]^+$ as well as radical cations, $[M]^+$. A strong molecular ion peak detected at m/z 649.31 is consistent to its proposed molecular formula.

The thermogravimetric analysis (TG) of the complex has been recorded in the nitrogen gas at a heating rate 10 °C min^{-1} over the temperature range of 50–600 °C. The complex decayed in three distinct steps. The first weight loss step of 14% takes place at ca. 150 °C corresponding to the loss of coordinated pyridine, followed by the second decomposition step corresponding to weight loss 43% which is attributed to the removal of aromatic moiety with imine linkage at temperature 151–300 °C. The aliphatic moiety attached with the metal ion, consistent with weight loss of 16% of total weight loss at 301–400 °C leads to the formation of U(VI) oxide as a final product in the third step. Finally, the remaining part left is uranyl oxide which is 27% of total weight.

3.2. Photoluminescence behaviour

The photoluminescence property of the complex was recorded at room temperature in ethanol.

The complex exhibited a prominent luminescent band at 470 nm upon excitation at 395 nm. However, there was noticed a slight bathochromic shift in the luminescence band position on comparing the spectra with uranyl acetate at the same excitation wavelength. The bathochromic shift observed is considered to be originated from the coordination of uranyl ion with the ligand.

4. Conclusions

A pyridine coordinated uranyl complex with distorted pentagonal bipyramidal geometry possessing U atom in the centre surrounded by UO_4N_3 bonds was investigated. The discussed complex exhibited significant fluorescence property in ethanol.

Acknowledgements

The authors would like to extend their sincere appreciation to the Deanship of Scientific Research at King Saud University for funding this work through Research Group number RG-1436-003.

References

[1] T.W. Hayton, J.M. Boncella, B.L. Scott, P.D. Palmer, E.R. Batista, P.J. Hay, Science 310 (2005) 1941.
[2] A.-C. Schmidt, F.W. Heinemann, W.W. Lukens Jr., K. Meyer, J. Am. Chem. Soc. 136 (2014) 11980.
[3] J.E. Niklas, B.H. Farnum, J.D. Gorden, A.E.V. Gorden, Organometallics 36 (2017) 4626.
[4] D. Hagberg, G. Karlstrom, B.O. Roos, L. Gagliardi, J. Am. Chem. Soc. 127 (2005) 14250.
[5] G. Szigethy, K.N. Raymond, Inorg. Chem. 48 (2009) 11489.
[6] R.G. Denning, J. Phys. Chem. A 111 (2007) 4125.
[7] J.M. Boncella, Nature 451 (2008) 250.
[8] H.-S. Hu, G.-S. Wu, J. Li, J. Nucl. Radiochem 31 (2009) 25.
[9] V.V. Atuchin, Z. Zhang, J. Nucl. Mater. 420 (2012) 222.
[10] Qing Lin Guana, Xue Gaoa, Jing Liuc, Wen Juan Weic, Yong Heng Xing, Feng Ying Baia, J. Coord. Chem. 69 (2016) 1026.
[11] S. Kannan, A.E. Vaughn, E.M. Weis, C.L. Barnes, P.B. Duval, J. Am. Chem. Soc 128 (2006) 14024.
[12] M. Sundararajan, A.J. Campbell, I.H. Hillier, J Phys Chem A 112 (2008) 4451.
[13] S. Tsushima, Inorg Chem 48 (2009) 4856.
[14] R. Nagaishi, Y. Katsumura, K. Ishigure, H. Aoyagi, Z. Yoshida, T. Kimura, Y. Kato, J. Photochem. Photobiol. A 146 (2002) 157.
[15] J.P. Corden, W. Errington, P. Moore, M.G.H. Wallbridge, Acta Cryst. C 52 (1996) 125.
[16] SAINT-Plus. Bruker AXS Inc., Madison, Wisconsin, USA. Bruker (2008).
[17] G.M. Sheldrick, Acta Crystallogr. A 64 (2008) 112.
[18] M. Azam, G. Velmurugan, S.M. Wabaidur, A. Trzesowska-Kruszynska, R. Kruszynski, S.I. Al-Resayes, Z.A. Al-Othman, P. Venuvanalingam, Sci. Rep. 6 (2016) 32898.
[19] D.L. Kepert, Prog. Inorg. Chem. 25 (1979) 41.
[20] F.H. Allen, Acta Crystallogr. B 58 (2002) 380.
[21] G.R. Desiraju, T. Steiner, The Weak Hydrogen Bond in Structural Chemistry and Biology, Oxford University Press, Oxford, 1999.

[22] R. Kruszynski, Acta Crystallogr Sect.C: Cryst. Struct. Commun. 65 (2009) o396.
[23] R. Kruszynski, T. Sieranski, Cryst. Growth Des. 16 (2016) 587.
[24] K. Nakamoto, Infrared and Raman Spectra of Inorganic and Coordination Compounds, Wiley, New York, 1986.
[25] L.J. Baucher, J. Inorg. Nucl. Chem. 36 (1974) 531.
[26] G.A. Kohawole, K.S. Patel, J. Chem. Soc., Dalton Trans. (1981) 1241.
[27] M. Asadi, K.A. Jamshid, A.H. Kyanfar, Inorg. Chim. Acta 360 (2007) 1725.
[28] M.A. Ryumin, Z.V. Dobrokhotova, A.L. Emelina, M.A. Bukov, N.V. Gogoleva, K.S. Gavrichev, E.N. Zorina-Tikhonova, L.I. Demina, M.A. Kiskin, A.A. Sidorov, I.L. Eremenko, V.M. Novotortsev, Polyhedron 87 (2015) 28.
[29] U. Casellato, S. Tamburini, P. Tomasin, P.A. Vigato, Inorg. Chim. Acta 341 (2002) 118.
[30] M. Shakir, M. Azam, Y. Azim, S. Parveen, A.U. Khan, Polyhedron 26 (2007) 5513.
[31] M.S. Refat, M.Y. El-Sayed, A.M.A. Adam, J. Mol. Struct. 1038 (2013) 62.
[32] M. Ulusoy, Özgül Birel, Onur Şahin, Orhan Büyükgüngör, Bekir Cetinkaya, Polyhedron 38 (2012) 141.
[33] H.C. Hardwick, D.S. Royal, M. Helliwell, S.J.A. Pope, L. Ashton, R. Goodacre, C.A. Sharrad, Dalton Trans. 40 (2011) 5939.
[34] M.S. Bharara, K. Strawbridge, J.Z. Vilsek, T.H. Bray, A.E.V. Gorden, Inorg. Chem. 46 (2007) 8309.